

## Seismic retrofitting of Fragavilla Monastery

Fillitsa V. Karantoni\*

*Department of Civil Engineering, University of Patras, Greece*

(Received October 28, 2012, Revised May 07, 2013, Accepted May 14, 2013)

**Abstract.** Practical seismic assessment and design of retrofit for the multitude of small ecclesiastical monuments that abound in the Balkans is the subject of this work. Application of the proposed procedures and methodologies are illustrated in an example case study, a small byzantine church located in Western Greece, which is the region with the highest seismicity in Europe. The church, known as the Fragavilla Monastery, had remained almost undamaged for 800 years, until 1993 when the Pyrgos earthquake caused critical damage mainly in the vaults. Linear elastic analysis to the recorded ground motion, capped by a biaxial failure criterion reproduced the developed damage. The same modelling and analysis procedure was subsequently used for assessment of the intended retrofitting measures. Proposed retrofitting measures included mitigation of the undesirable implications of past interventions along with a combination of strengthening schemes with externally bonded AFRPs strategically placed in the structure. The effectiveness of the proposed solutions is gauged by successful reduction of stress intensity in the critical regions and mitigation of stress localization throughout the structure.

**Keywords:** brickwork and masonry; load bearing masonry; historical buildings, structures and design; conservation; restoration

### 1. Introduction

A considerable number of small domed byzantine churches, which were erected circa 1200 A.D. is spread all over the Balkan region. Over three hundred of them are scattered all over Greece; they are located throughout the country, in urban or even in remote rural areas; some are in good structural condition whereas others are heavily damaged due to exposure to extreme weather events, earthquakes, soil corrosion and settlement through their long-lasting existence. Despite some common structural characteristics, each church is unique because of the local tradition in workmanship, the skill of the masons, the available materials and the special characteristics of the site where they have been erected.

Although ecclesiastic monumental structures have been the object of extensive study throughout Europe, rural byzantine churches have received little attention by structural engineers. This lack of attention is particularly troubling in light of the considerable seismic risk in the Balkan Peninsula rendering the need for assessment, seismic retrofitting and preservation of this important architectural heritage a pressing societal priority.

In this paper the issue of seismic assessment and definition of a retrofit strategy is explored

---

\*Lecturer, E-mail: [karmar@upatras.gr](mailto:karmar@upatras.gr)

systematically, using an example case study for demonstration of concepts. As it is mentioned in the section 3, the damage of load bearing walls was limited and this is the reason the present paper is focused on the strengthening of damaged vaults. The structure is a damaged byzantine church known as the Fragavilla Monastery that was built in the 1200's. It is located in Western Peloponnese (Greece) and remained almost undamaged for eight centuries. Due to the 1993 Pyrgos earthquake, critical damage occurred in the church and repair and strengthening were deemed mandatory. During emergency protection measures against further damage, important archaeological findings gave rise to additional concerns: earlier structural interventions, most likely intended to control differential settlements had been implemented at an unknown past, and therefore their implications on the seismic response of the church would have to be accounted for. It is noteworthy that archaeological works did not execute below the ground level.

The methodology used for dynamic analysis of the structure in its various phases relied on linear elastic finite element modelling and simulation. Note that modelling for this class of historical structures is hampered by several uncertainties, such as: (a) lack of knowledge about the actual state and mechanical properties of the materials particularly in light of the aging process over the past 800 years, and the combined deterioration owing to corrosion and erosion and biological breakdown of mortar, masonry units and timber, (b) inadequate understanding of the degree of cooperation between different materials, particularly at the interfaces between timber lacing and stone or mortar, and between stone foundation and the soil, (c) imperfect interaction imparts an unknown, indeterminate degree of fixity at the points of contact, a feature that poses demands for more complex and detailed modelling than what is conventionally used in order to credibly account for all the important mechanisms that control the actual response of the structure.

In the present investigation, equivalent linear static analysis was conducted using the total acceleration response spectra of site acceleration histories recorded nearby. Results obtained from the analysis are in good correlation with the observed damage patterns confirming the relevance of the adopted modelling procedures. The implications on the seismic performance of the church owing to structural interventions implemented in the past were examined. It was shown that the structure in its original state was less vulnerable than the structure "as was" at the time when the earthquake occurred; restoration back to the "original" state was deemed appropriate. This step was therefore considered a prerequisite to further retrofit options.

## **2. Description of the church case study – structural details**

The church is of the "cross-in-square" type; the cylindrical drum is based at the crossing of longitudinal and transept barrel vaults. The drum supports the dome, which is also carried by pendentives (Fig. 1(b), parts 5-8). The four "corner bays" transform the plan into an orthogonal of dimensions  $10.10 \times 9.10$  m, as shown in Fig. 1(a). During the long life of the monument, the main vaults, identified with numbers 1 to 4 in Fig. 1(b), as well as parts of the vaults of the corner bays were covered with layers of normal and lightweight gravel. For this reason, the walls which support the vaults were built up higher than the level of their extrados as illustrated in the perspective drawing of Fig. 2(a). Because of this intervention, the lower half part of the cylindrical drum which supports the dome was buried, effectively confined by the gravel pressures through the depth of the gravel fill. The two pairs of buttresses placed transversely to the external aisle walls are also interventions of an earlier period with an obvious intention to prevent the outwards movements of the north and south walls due to the thrust imparted by the dome. The thicker west

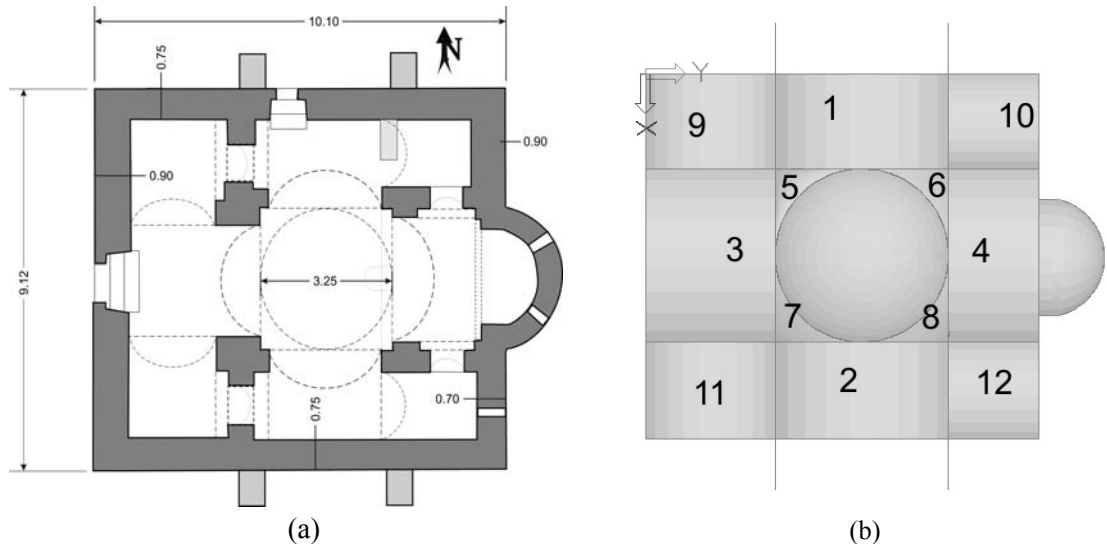


Fig. 1 The Fragavilla Monastery church, (a) floor plan, and (b) nomenclature of the architectural features

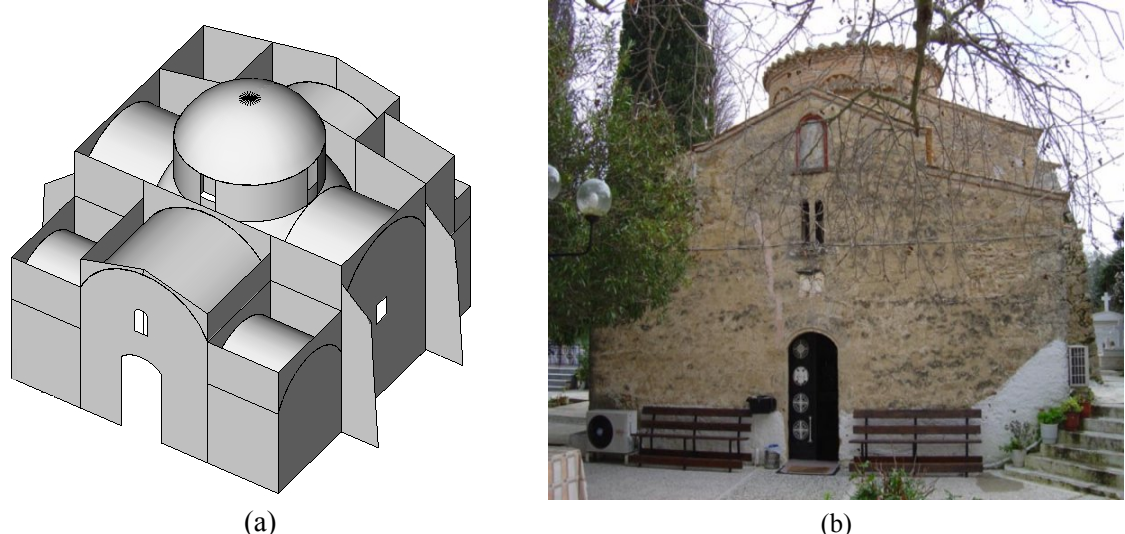


Fig. 2 (a) Perspective drawing of the church "as was" (IS Model) during the earthquake, and (b) a picture taken from west before the 1993 earthquake

wall and the direction of vaults of west corner bays reduce the thrust there, whereas the existence of apse at east reduces the span of east wall, so it seems that the period of interventions there was no need for buttressing the west and east walls.

Old sealed cracks on the north and west external walls reveal the earlier presence of differential settlements of the walls, which are believed to have occurred in an unknown past, the most severe damage being on the west façade wall Fig. 2(b). A relevant geotechnical study confirmed that the stiff clay under the stone foundation provided adequate load bearing capacity, a finding inconsistent with the inference that attributed cracking to differential settlement. Note however

that according with a local legend, the church had been built over the ruins of an older church, which may account for the settlements and the consequent past interventions. To the author's opinion it seems that the extended parapets over the load bearing walls, with increasing height from the west to the east intended to accommodate the normal and lightweight gravel fill, had been constructed in order to control the settlement of the western part of the structure: the progressive increase of vertical loads from the west to the east was expected to reduce or even to stop the differential settlement in progress. The increasing of vertical loads from west to east increases linearly the settlements so that the settlement became uniform and thus there is not differential but uniform settlement. Note that a primary finding of the study, based on the type of masonry work in that segment, is that the western main vault had been rebuilt at an unknown earlier period.

The external load bearing walls with variable thickness ranging from 0.70 m to 0.90 m were constructed of uncoursed porous lime stones. Large, hewn cornerstones still provide good connection between orthogonal walls and as a result no separation of the adjacent walls has occurred due to the repeated earthquakes that the church had sustained over its 800 year long life. The interior walls, the four pillars, the vaults, the pendentives and the dome are made of solid bricks of a relatively large length as illustrated in Figs. 2 and 3. Both the dome and the vaults have a thickness of 0.26 m. The shallow foundation is a typical one for this class of structures, whereby the walls are extended into the ground by about 1.0 m.

### **3. Description and diagnosis of the state of damage**

The interventions at the top of the vaults as well as the addition of the buttresses are signs that damage had developed over the centuries of the monument's life and they were intended to prevent the church from further devastation. In 1988, the Vartholomio earthquake of  $Ms = 5.9$  with an epicentre of about 40 km away from the monastery's location, caused some cracking but did not disturb the integrity of the structure. However, in the earlier event of the 1993 the Pyrgos earthquake critical damage had occurred in the monument and shoring had been required to prevent it from collapse. All structural members of the monument, except the stiff external walls, had developed cracking. The most important damage observed was the downwards and southwards movement of the south transept which was manifested by, (a) detachment from the dome and the south wall, as illustrated on the left of Fig. 3 and, (b) eastwards movement of the eastern vault which created a crack of about 10cm. Longitudinal cracks developed also in the vaults of the east-corner bays, which were overburdened by the gravel fill. Due to this deformation, minor cracks had been formed in the internal walls that connect the piers but also in the four central piers that support the dome. The recorded damage of the north main vault (vault 1 in Fig. 1(b)) is shown in Fig. 4. Detailed drawings of the cracking patterns of the vaults are provided in Karantoni (2010).

### **4. Modelling procedures**

#### *4.1 Modelling of the structure*

The structure was discretized using a large number of triangular and rectangular isoparametric shell finite elements in order to account both for in-plane and out-of-plane response. 4-noded shell



Fig. 3 The South East pendentive (part 8 - the light-coloured region was buried by the infill)



Fig. 4 The north main vault (part 1)

elements provided in the element library of ACORD-CP were used. The thickness of each shell element equals that of the corresponding structural component being modelled. The buttresses are also simulated using shell elements. The nodes of the finite elements have six degrees of freedom except those at the foundation level which considered to be fixed. Because the available drawings document the church in its current, deformed state, any deviation from the vertical was taken into consideration in defining the geometry of the model. Since no damage was developed in external walls where the vaults impose eccentricities, this effect in the actual structure must have been minor, and for this reason one is encouraged to think that its omission in the model may not have caused significant uncertainty to the relevance of the results. Assumptions made for the material properties and the seismic loading are evaluated through the ability of the model to reproduce the observed patterns of damage (*model verification stage*); such values as verified through this process, are subsequently used in a follow-up analysis for performance estimation of the proposed retrofit measures (*response estimation stage*).

#### 4.2 Mechanical properties of the masonry

Since there were no experimental data available for strength and deformation characteristics of the structure's masonry elements, material properties were obtained from published empirical formulae. It was assumed that the interior leaf of the three leaf uncoursed masonry of porous lime

stone contains a high volume ratio of lime mortar and therefore the density of the composite stone masonry was taken equal to  $2100 \text{ kg/m}^3$ . The density of solid brick masonry of the interior walls, the vaults and the dome was taken equal to  $1800 \text{ kg/m}^3$ . The masonry was modeled as an elastic isotropic material, a common hypothesis for structures of uncoursed masonry, e.g., as in Pengon *et al.* (1995) and Triantafillou & Fardis, (1997). Uniaxial compressive strength of stone masonry was  $f_w = 1.8 \text{ MPa}$  and of brick masonry  $f_w = 2.93 \text{ MPa}$ , (Karantoni 2008, 2010). Accordingly, the modulus of elasticity was taken as  $E = 1000f_w$ , i.e., 20% lower than the proposed nominal value (Tassios and Chronopoulos 1986) in order to account for the light extent of existing cracking. The Poisson's ratio was taken  $\nu = 0.20$ .

#### 4.3 The seismic hazard

The seismic excitation of March 26 1993 consisted of three strong ground motions with epicenters located  $5 \div 20 \text{ km}$  away from the Monastery of Fragavilla (near fault ground motions). The critical shock at the site of the monument was the seismic event at 12:56 on the 26<sup>th</sup> of March ( $M = 5.1$ ) recorded at AMAL station, 2 km to the NW from the church location, with a ground peak acceleration in the NW-SE of 0.46 g according to Stavrakakis (1996). From the ground motion record in the transverse direction which is presented in Fig.5 (see (ISESD) archives, <http://www.iseds.cv.ic.ac.uk>), the demand in terms of spectral total acceleration was found to be 0.12 g for the fundamental period of the church,  $T = 0.09 \text{ sec}$  (Karantoni 2002) and damping 20% which is reasonable for masonry structures. Linear equivalent static analyses were performed for gravity loads and eight seismic load combinations;  $G \pm E_x \pm 0.30E_y$  and  $G \pm 0.30E_x \pm E_y$  with the seismic loads  $E_x$  and  $E_y$  representing the horizontal seismic forces taken equal to 0.12g the mass of the structure, distributed along the height of the structure according with an inverse triangular pattern. The triangular distribution was chosen so as to be consistent to seismic codes in force, since the distribution according to modal shape is not representative because minor part of mass is vibrating, especially after the strengthening measures, as it is mentioned in the next.

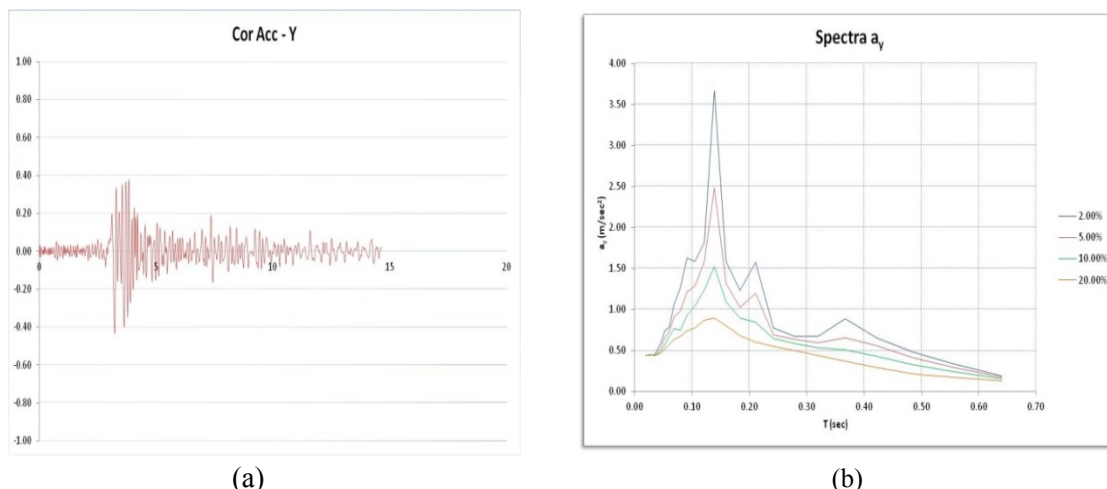


Fig. 5 The y- component of the corrected acceleration time history recorded nearby the Monastery (a); and the corresponding elastic response spectrum (b) (Data from National Observatory of Athens)

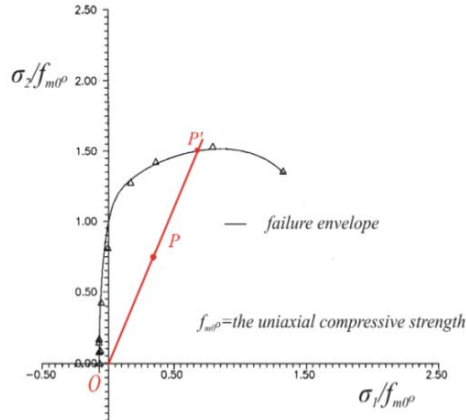


Fig. 6 The proposed failure envelope

#### 4.4 Criterion for masonry failure

In conducting the simulations a plasticity-based isotropic constitutive model was used to evaluate the stress-strain behaviour of stone-masonry walls under plane stress. Note that several alternative biaxial failure envelopes have been proposed for masonry under plane stress, intended to account for the semi-brittle and tension-deficient behaviour of the material (e.g., Page 1981, Mann and Müller 1986, Dialer 1991, Lourenço 1996, Zucchini and Lourenco 2004, Calderini and Lagomarsino 2006, Christensen 2004, among others). A relevant model proposed by the author is used in the present work to account for material failure in Karantoni *et al.* 1993. The model was obtained after calibration of the well-established Ottosen's four-parameter failure envelope (intended for semi-brittle materials), with a large database of biaxial tests conducted on brick masonry wallettes, where the angle forming between the directions of principal tension and that of the masonry bed joints was a parameter of study in correlating the parameters of the criterion. The failure envelope for idealized isotropic masonry under triaxial stress conditions is defined by Ottosen 1997

$$\alpha \frac{J_2}{f_w^2} + \lambda \frac{\sqrt{J_2}}{f_w} + \beta \frac{I_1}{f_w} = 1 \quad (1)$$

where  $I_1$  is the first stress invariant and  $J_2$  is the second deviatoric stress invariant. Parameter  $\lambda$  depends on the inclination of the octahedral plane,  $\theta$

$$\lambda = c_1 \cos \frac{\cos^{-1}(c_2 \cos 3\theta)}{3} \quad \text{if } \cos 3\theta \geq 0 \quad (2)$$

$$\lambda = c_1 \cos \frac{\pi - \cos^{-1}(-c_2 \cos 3\theta)}{3} \quad \text{if } \cos 3\theta < 0 \quad (3)$$

where

$$\cos 3\theta = \frac{3\sqrt{3} J_3}{2J_2^{3/2}} \quad (4)$$

Note that  $\theta = 60^\circ$  for uniaxial compression,  $\theta = 0^\circ$  for both uniaxial tension and biaxial compression, and  $J_3$  is the third deviatoric stress invariant. Also

$$\beta = \frac{1}{3} \left( \frac{1}{f} - \frac{1}{b} + \frac{b-f}{3} a \right) \quad (5)$$

Parameter  $a$  in equations 1 and 5 is a function of the stress condition (Karantoni *et al.* 1993) and  $f$  is the ratio of tensile to compressive strength of masonry, whereas  $b$  is the strength ratio under symmetric biaxial compression; best-fit calibration with the available experimental database is obtained for  $b = 1.65$  and  $f = 0.085$ .

In the stress space defined by the two orthogonal principal stress axes, an arbitrary stress state having stress coordinates  $\sigma_1, \sigma_2$ , is represented by the point P (Fig. 6). This stress state is evaluated with respect the failure envelope by considering the length of the radius OP', going through P, to the failure envelope to point P'. If the ratio OP/OP' is denoted by  $\sigma^*$ , then, normalizing the stresses by  $\sigma^*$  would produce a stress state,  $\sigma_1/\sigma^*, \sigma_2/\sigma^*$  that lies exactly on the failure envelope. (Thus, the pair  $(\sigma_1/\sigma^*, \sigma_2/\sigma^*)$  satisfies the equation of the criterion). In this light, practically  $\sigma^*$  is a safety factor: stress combinations values with  $\sigma^* < 1$  lie inside the failure envelope, whereas cases having  $\sigma^* > 1$  have reached plastification, which, in masonry is associated conceptually with failure due to the apparent brittleness of the material.

## 5. Evaluation of the modelling assumptions

The finite element model representing the church “as was” when struck by the 1993 earthquake comprised 4355 finite elements and 2340 nodes – it is referred to hereon, as model IS (initial state). Modal and equivalent static analyses were performed according with the assumptions outlined in the previous section. Modal analysis revealed higher deformations when the structure is vibrating along the x axis. Furthermore, it was shown that 67% of the mass participates in the fundamental modes along the x and y axes; these modes are strongly marked by out of plane bending deformation components; the two translational fundamental modes in the x and y directions are shown in Fig.7. Upon comprehensive evaluation of the results of linear equivalent static analysis it was concluded that the analytical estimations were consistent with the observed damage. No damage was anticipated in the external walls under any of the eight different seismic load combinations considered in the analysis, consistently with the field observations. Field reports of damage in the vaults were in agreement with the findings of the analysis. Actually, the analytical estimates successfully identified not only the location but the orientation of cracking as well (Karantoni 2008, 2010). This is illustrated when comparing the damage pattern of the south-east pendentive shown in Fig.3 with the estimated contours of  $\sigma^*$  for the loading combination G-0.30E<sub>x</sub>-E<sub>y</sub> as depicted in Fig.8 (a). Table 2 lists the value for the peak equivalent stress  $\sigma^*$  calculated over either of the two faces of the masonry wall, i.e. either on the extrados or the

intrados of the vault. The mean value of  $\sigma^*$  at the main vaults (i.e. parts 1-4) is about 3.5, for the pendentives (parts 5-8) and the corner bays (parts 9-12) it is 5.9 and 3.4, respectively. Note that the max  $\sigma^*$  for gravity loads equals 0.96 and it occurs at intrados at the base of the drum; thus, the stress-state in the masonry at this location is near failure.

## 6. Retrofitting measures

### 6.1 Removal of parapet walls and infill

Under gravity loads the added vertical pressure provided by the infill partly counteracts the horizontal thrust of the reaction force developing at the spring of the vaults. The influence of this pressure on the seismic response of the structure in consideration was studied using a modified F.E. model of the structure in its original condition (i.e., after removal of the interventions used in the IS model; this, revised model, is referred to as OC in the following discussion). A perspective drawing of the structure in that state is shown in Fig.9. A short while before this study, the external stone masonry walls had been repointed with a lime grout. This modification was accounted for in the model by assigning pertinent values to the mechanical properties of the continuum that represented stone masonry in the F.E. model. Values for these properties had been obtained through testing of similarly constructed and grouted masonry wallettes (Vintzileou & Miltiadou 2008). According to this study, grout injection of masonry with a lime grout that would be compatible with the stone masonry (mimicking the historical grouts used at the time of construction of the church) could increase the compressive strength of stone masonry (mimicking the historical grouts used at the time of construction of the church) could increase the compressive strength of stone masonry by about 50%. The mortars of historical structures are mainly lime sand mortars which also have compounds with hydraulic activity such as pozzolana and brick powder (Karaveziroglou *et al.* 1985). On the contrary, the compressive strength of the clay brick masonry

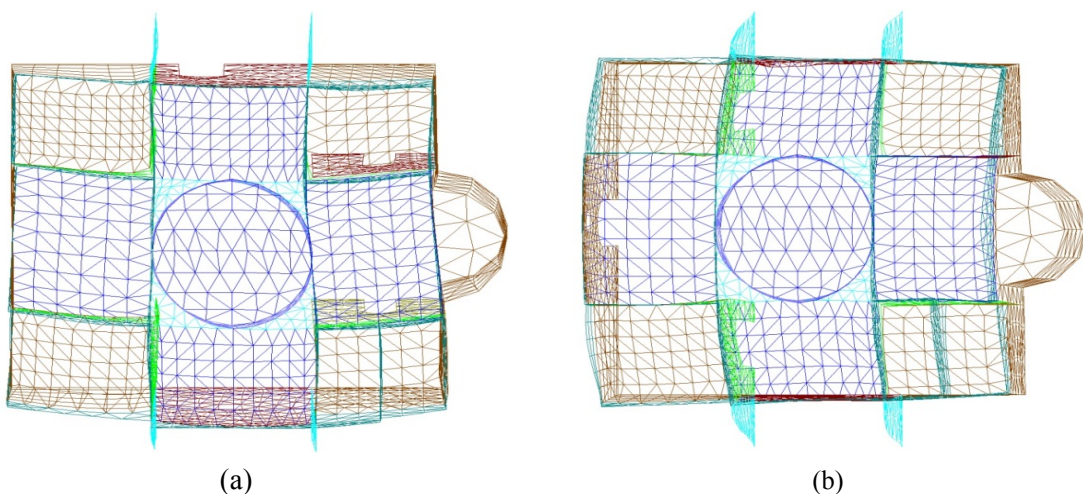


Fig. 7 The fundamental eigenmodes obtained from the IS Model for translation in a) the x, and b) the y axis, respectively

Table 1 Periods and percentage of participated mass (M.P.F) in the first ten eigenmodes

Mode	Period (sec)	M.P.F along x (%)	M.P.F along y (%)
1	0.086	67.33%	0.01%
2	0.079	0.01%	67.89%
3	0.062	0.04%	0.35%
4	0.053	0.01%	0.00%
5	0.053	0.00%	0.18%
6	0.051	0.65%	0.01%
7	0.049	0.01%	0.48%
8	0.047	0.01%	0.00%
9	0.039	0.06%	0.44%
10	0.037	0.05%	1.40%

Table 2 Max equivalent stress  $\sigma^*$  developed at the vaults of the structure “as was” during the earthquake, regardless of the face developed

Part	G	G+ $E_x+0.3E_y$	G+ $E_x-0.3E_y$	G- $E_x+0.3E_y$	G- $E_x-0.3E_y$	G+ $0.3E_x+E_y$	G+ $0.3E_x-E_y$	G- $0.3E_x+E_y$	G- $0.3E_x-E_y$
1	0.96	5.13	3.17	2.90	3.96	3.80	2.58	3.75	3.96
2	0.96	2.92	3.62	4.83	3.19	2.68	3.81	4.01	3.69
3	0.59	4.98	3.34	5.42	3.35	3.59	3.89	3.19	3.20
4	0.87	2.40	3.05	2.40	3.14	3.16	3.35	2.73	2.67
5	0.72	11.0	5.97	7.70	10.40	9.12	5.79	7.28	8.95
6	0.54	4.14	5.05	4.81	4.83	4.29	4.53	4.65	3.50
7	0.65	6.35	6.90	9.11	6.21	3.36	6.76	6.72	4.96
8	0.96	3.41	3.44	4.00	5.00	5.43	5.37	4.04	4.81
9	0.47	4.43	3.19	3.50	4.40	3.57	3.19	3.00	3.78
10	0.63	3.91	3.63	4.16	3.83	2.47	3.13	3.74	3.03
11	0.39	3.07	3.77	4.43	3.28	3.12	3.57	3.68	2.95
12	0.58	3.09	3.14	3.16	2.90	2.75	1.78	2.77	3.05

used in the vaults was assumed to be reduced to 85% of the previously calculated value, to account for compression softening of the material when accounting for the extent of damage, regardless of possible sealing or stitching of the cracks, with a commensurate reduction of the material stiffness moduli. In light of these hypotheses, compressive strengths of 2.7 MPa and of 2.5 MPa were assigned to stone and brick masonry, respectively.

The implications of the model alterations may be gauged immediately from the effected differences in the fundamental modes of vibration and the distribution and magnitudes of the equivalent stresses  $\sigma^*$ . The fundamental lateral translational modes in the two orthogonal directions of the plan are depicted in Fig. 10; these are compared with their counterparts shown in Fig. 7. The structure responds uniformly, regardless of the direction of excitation. The first mode in the x direction has the highest degree of mass participation (24% of the total translational mass);

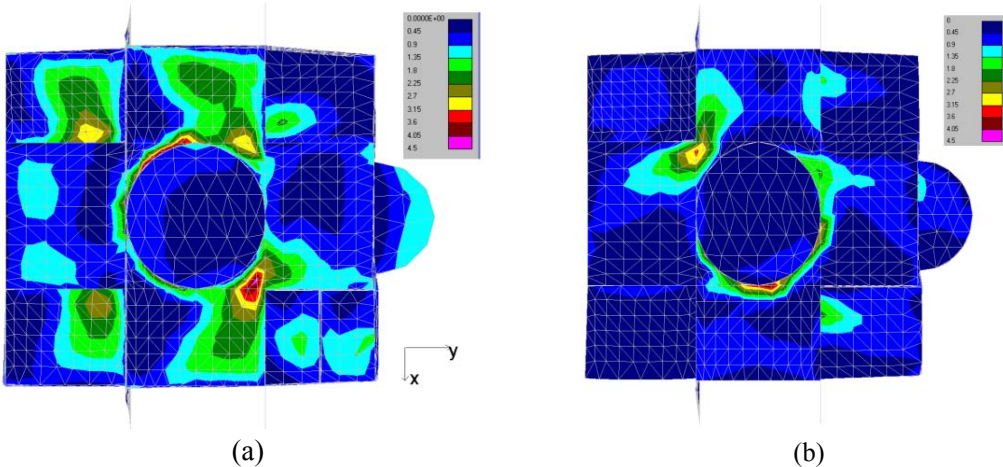


Fig. 8 Contours of  $\sigma^*$  at the intrados for loading combination G-0.30Ex-Ey of the structure: (a) IS Model, and (b) OC Model

however along the y axis none of the first ten modes can mobilize a significant amount of the translational mass of the structure. The values of maximum equivalent stress  $\sigma^*$  over the two faces of masonry are listed in Table 3, for comparison with the corresponding values in Table 2. Note that the mean value of  $\sigma^*$  at the main vaults is about 3.3 and at the pendentives and the corner bays 4.9 and 1.7 respectively, which corresponds to a reduction by 6%, 17% and 50%, from those attained by the structure “as was” during the 1993 Earthquake (i.e., values from IS model, prior to the removal of the fill). Although the reduction in the maximum equivalent stress  $\sigma^*$  is not significant, the regions in the vaults developing values that lie outside the failure envelope, i.e., with  $\sigma^* > 1$ , are restricted affecting significantly reduced regions in the OC model as compared to the IS model of the structure. Indicatively, it may be seen in Fig. 8(b) that for the loading combination G-0.30E<sub>x</sub>-E<sub>y</sub>, the area of the region affected with  $\sigma^* > 1$  in the OC model is reduced in comparison with the corresponding region of the structural model IS, illustrated in Fig. 8(a). Clearly, upon restoration of the church to its original form, with sole intervention measure being an increase of the masonry strength through good quality grout injection of stone masonry, the maximum values of  $\sigma^*$  remain still high, as was expected because the clay masonry of the vaults is not grouting and therefore, additional retrofit would still have to be planned in order to mitigate the risk of damage in the critical elements of the structure under the design earthquake.

## 6.2 Strengthening through EBR-AFRPs at the extrados of the main vaults

The existence of frescos in the church interior prohibits any intervention at the intrados except the sealing of cracks which has already been taken in consideration during modelling where an un-cracked structure was supposed. Considering the critical cracking, it is reasonable not to reject any of the so called modern retrofitting techniques such as confinement through externally bonded FRP sheets (EBR-FRPs), if the interior appearance of the church must remain unaffected after the implementation. Note that the tile roofing may completely cover the intended external intervention at the extrados of the vaults (Mazzolani & Mandara 2002, Valluzzi & Modena 2001, Tararu *et al.* 2010). In this section, strengthening the vaults 1 to 8 (as illustrated in Fig. 1(b)), through externally

bonded Aramid Fibre Reinforced Polymer sheets at their extrados, is explored as a possible retrofit solution. Multi-ply aramid sheets of 2.0mm in total thickness is considered perfectly bonded on the extrados, thereby providing a two layer material; the inner layer of 0.26m thickness is the masonry structure, with the mechanical properties given in Section 6.1, whereas the outer layer comprises 0.002 m thick, bi-directional Aramid sheet with a Young's modulus  $E = 90\text{GPa}$  and a Poisson's ratio of  $\nu = 0.35$ . The analytical model of the FRP-retrofitted structure is referred to as ExFRP1 mode and is obtained from the OC model after introduction of the properties and element geometry affected by the ExFRP. The estimated reduction of the maximum equivalent stresses  $\sigma^*$  for each one of the twelve structural parts of Fig. 1(b), is listed in Table 4. For the purposes of comparison the corresponding stresses of Table 3, calculated for the OC model, are shown. If good execution of the strengthening application is secured and sufficient anchorage is provided at the edges of the wraps so that the mathematical model may be representative of the actual boundary conditions, a reduction of  $\sigma^*$  by up to 90% was predicted for some loading combinations. In more

Table 3 Max equivalent stress  $\sigma^*$  developing in the vaults of the OC model (on either face of the member)

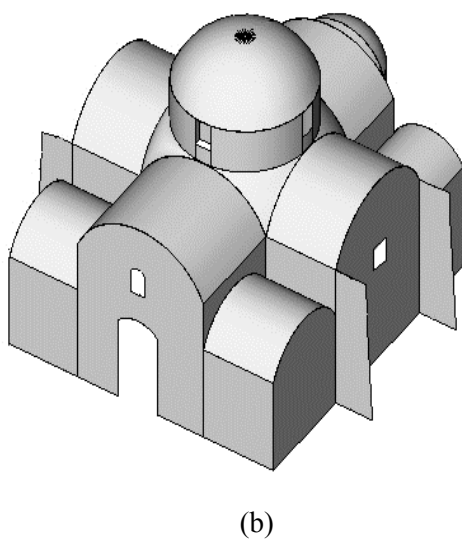
Part	G	G+ $E_x+0.3E_y$	G+ $E_x-0.3E_y$	G- $E_x+0.3E_y$	G- $E_x-0.3E_y$	G+ $0.3E_x+E_y$	G+ $0.3E_x-E_y$	G- $0.3E_x+E_y$	G- $0.3E_x-E_y$
1	1.13	5.08	4.66	3.75	4.10	3.00	2.48	1.80	2.33
2	1.13	3.53	3.27	3.91	4.15	2.86	2.66	2.49	2.85
3	0.89	2.70	2.61	2.12	3.18	4.11	3.63	3.98	4.25
4	0.96	1.99	2.42	2.03	2.40	4.52	4.80	4.82	4.56
5	0.93	5.80	4.39	3.10	5.40	6.17	4.28	4.02	5.90
6	1.06	4.08	5.14	4.12	3.21	4.71	5.79	6.18	5.33
7	0.77	3.26	5.70	5.15	4.08	5.57	5.96	5.73	4.83
8	0.69	3.83	2.88	3.63	4.83	5.65	5.04	5.76	6.30
9	0.32	1.65	1.31	1.57	2.19	1.87	1.48	1.55	1.94
10	0.49	2.10	2.60	1.74	1.52	1.33	1.89	1.96	1.06
11	0.39	1.55	2.04	1.56	0.99	1.82	2.20	1.89	1.38
12	0.39	1.73	1.45	1.95	2.36	1.86	1.48	0.76	1.69

detail, the mean value of the maximum  $\sigma^*$  over the two faces of masonry is reduced to 1.32, 1.47 and 0.60 which represent a reduction of  $\sigma^*$  for all eight seismic combinations by 58%, 70% and 64% on average, for main vaults, the pendentives and the vaults of corner bays, respectively. The average reduction is 64% concerning all the vaults under the eight seismic loading combinations. The technique affects much more the pendentives which are the most vulnerable parts and it is also effective in reducing the stress state at the corner bays although no direct intervention was considered for these locations. The estimated contours of  $\sigma^*$  at the intrados of the masonry layer are shown in Fig. 11 for comparison, obtained for the relevant loading combination of Fig. 8. In more detail, the mean value of the maximum  $\sigma^*$  over the two faces of masonry is reduced to 1.32, 1.47 and 0.60 which represent a reduction of  $\sigma^*$  for all eight seismic combinations by 58%, 70% and 64% on average, for main vaults, the pendentives and the vaults of corner bays, respectively. The average reduction is 64% concerning all the vaults under the eight seismic loading

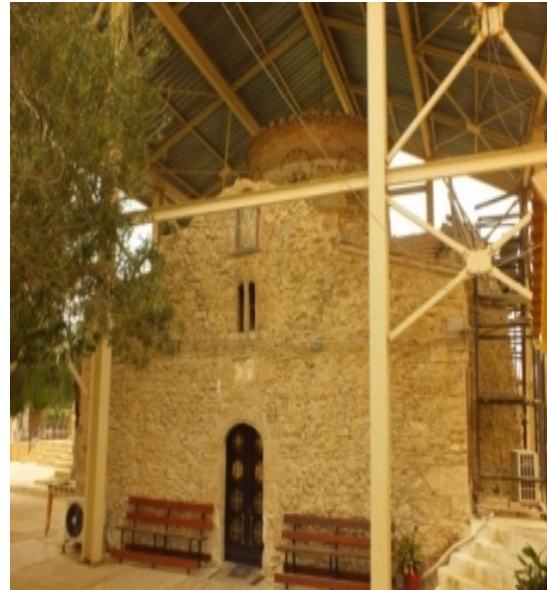
Table 4 Reduction of max  $\sigma^*$  regardless of the face developed, from the Ex-FRP1 version of the OC Model

Part	G	G+ $E_x+0.3E_y$	G+ $E_x-0.3E_y$	G-E <sub>x</sub> +0.3 E <sub>y</sub>	G- E <sub>x</sub> -0.3E <sub>y</sub>	G+ 0.3E <sub>x</sub> +E <sub>y</sub>	G+ 0.3E <sub>x</sub> -E <sub>y</sub>	G-0.3E <sub>x</sub> + E <sub>y</sub>	G- 0.3E <sub>x</sub> -E <sub>y</sub>
1	7%	55%	61%	88%	90%	31%	40%	27%	61%
2	17%	85%	80%	59%	60%	66%	47%	48%	41%
3	23%	56%	68%	53%	83%	61%	61%	88%	88%
4	-19%	18%	13%	64%	43%	79%	80%	29%	35%
5	43%	70%	64%	75%	94%	66%	57%	80%	90%
6	34%	54%	59%	91%	76%	80%	89%	61%	61%
7	26%	58%	89%	50%	44%	53%	56%	83%	80%
8	34%	77%	76%	41%	43%	87%	88%	70%	62%
9	43%	54%	57%	83%	91%	61%	66%	85%	91%
10	45%	80%	80%	87%	84%	87%	92%	73%	61%
11	4%	65%	68%	31%	38%	39%	39%	66%	72%
12	5%	60%	68%	45%	43%	62%	64%	17%	35%

combination. The technique affects much more the pendentives which are the most vulnerable parts and it is also effective in reducing the stress state at the corner bays although no direct intervention was considered for these locations. The estimated contours of  $\sigma^*$  at the intrados of the masonry layer are shown in Fig. 11 for comparison, obtained for the relevant loading combination of Fig. 8.



(b)



(b)

Fig. 9 Perspective drawing of the “original” church (OC Model) (a), and a recent picture of the church which is protected from the rainfall by an external steel structure (b)

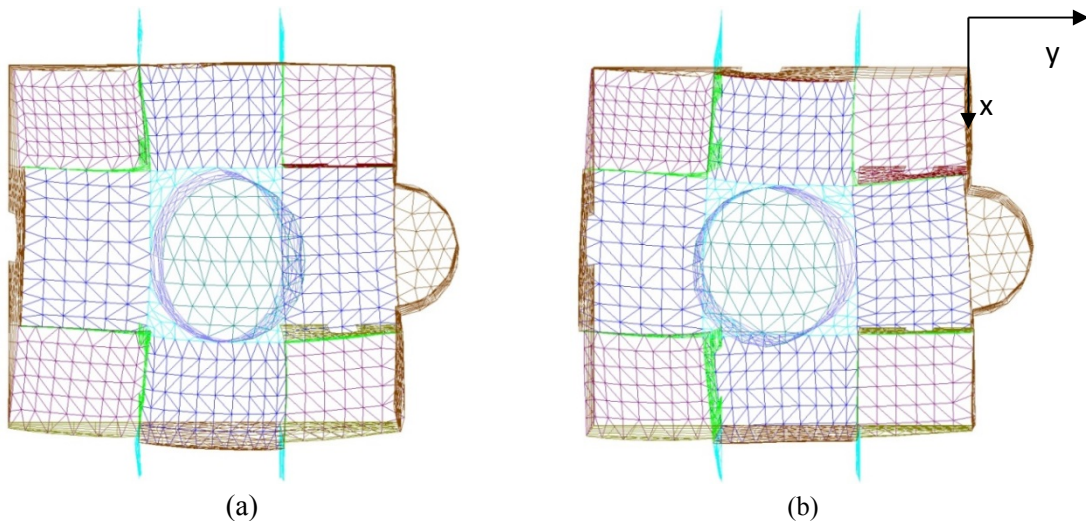


Fig. 10. The fundamental eigenmodes of the OC Model along a) the x and b) the y axis, respectively

### *6.3 Bonding of AFRPs at extrados of all the vaults*

In order to investigate the probable additional benefits from bonding AFRPs at all the vaults, the vaults 1 to 12 in Fig. 1(b) were modelled assuming a two layer material, with the properties mentioned in Section 6.2. The structural model obtained in this manner is referred to hereon as ExFRP2. The effected reduction in  $\sigma^*$  relative to that of the original structure is listed in Table 5 as a percentage of the associated OC value. The mean value for the maximum  $\sigma^*$  over the two faces of masonry is reduced to 1.36, 1.60 and 0.28 which represent a percent reduction of  $\sigma^*$  by 56%, 67% and 82% on average for all eight seismic combinations, for the main vaults, the pendentives and the vaults of corner bays, respectively. It is noteworthy that when compared to

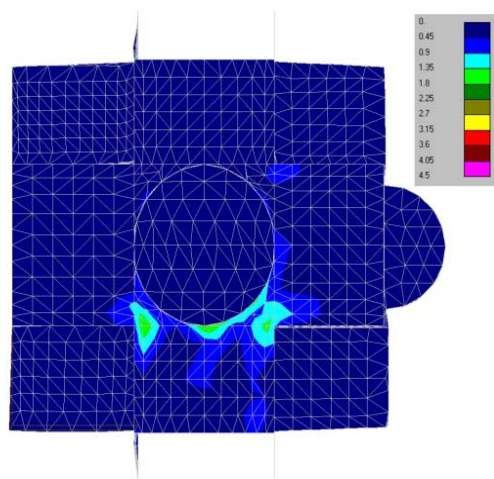


Fig. 12 Contours of  $\sigma^*$  for load combination G-0.30Ex-Ey at intrados of the ExFRP2 Model (AFRP bonding on all vaults)

Table 5 Reduction of max  $\sigma^*$  regardless of the face developed, from the model Ex-FRP2 as compared with the OC structure

Part	G	G+ E <sub>x</sub> +0.3E <sub>y</sub>	G+ E <sub>x</sub> -0.3E <sub>y</sub>	G- E <sub>x</sub> +0.3E <sub>y</sub>	G- E <sub>x</sub> -0.3E <sub>y</sub>	G+ 0.3E <sub>x</sub> +E <sub>y</sub>	G+ 0.3E <sub>x</sub> -E <sub>y</sub>	G- 0.3E <sub>x</sub> +E <sub>y</sub>	G- 0.3E <sub>x</sub> -E <sub>y</sub>
1	2%	48%	56%	86%	88%	18%	29%	24%	60%
2	11%	82%	80%	53%	53%	59%	37%	45%	35%
3	26%	54%	64%	53%	82%	58%	59%	86%	85%
4	-7%	24%	15%	54%	48%	81%	82%	49%	55%
5	44%	68%	62%	76%	91%	63%	56%	80%	87%
6	34%	51%	57%	87%	77%	80%	87%	57%	58%
7	25%	58%	85%	45%	39%	51%	54%	78%	77%
8	33%	72%	73%	37%	39%	84%	85%	67%	59%
9	43%	68%	65%	92%	95%	75%	75%	83%	91%
10	60%	81%	82%	90%	89%	89%	94%	80%	75%
11	72%	91%	94%	74%	70%	85%	82%	92%	88%
12	43%	88%	86%	79%	78%	93%	91%	46%	72%

the previous case, this extra cost in the intervention, as expected, is rather effective in protecting the vaults of the corner bays, but provides little benefit for the other parts (see also Fig. 12). Taking into account that the mean value of max  $\sigma^*$  over the corner bays for all the eight seismic combinations is reduced from 0.60 to 0.28 one may conclude that bonding of ExFRPs at the external surface of vaults of corner bays would not be essential for improving the overall response.

## 7. Conclusions

Despite the scarcity in test data concerning the mechanical properties of masonry, the consistent assumptions made in assembling the finite-element model of the historical monument can faithfully reproduce the effects of strong ground motions with particular reference to the extent of damage. This method is examined in the present study in order to guide diagnosis, assess a variety of retrofit solutions and enable design of the strategic retrofit using a medieval byzantine church as an object of study (case study). The most vulnerable structural elements were identified as the base of the drum and the pendentives. The structural interventions implemented at an unknown past which consisted of addition of dead weights to the structure (gravel fill) at gradually increasing depths from the west to the east in order to control differential settlements were shown to be beneficial to permanent loading but proved critical under seismic loading due to the eccentricity and large inertia they generated. Modern techniques, such as bonding of polymer sheets at the extrados of the vaults, were modelled and analyzed and calculated results were very encouraging because they were effective in reducing the stress demand in the critical locations. They are advantageous as they do not burden the structure with weights, while remaining invisible when covered under the tile roof. When applying ExFRPs (aramid) on both the main vaults and the pendentives, a reduction of the maximum equivalent stress  $\sigma^*$  by about 65% on average was estimated when considering all the vaults for eight seismic load combinations. Extending the

technique to the vaults of corner bays affected only the relevant parts although they were not deemed necessary for improving the overall structure.

## References

- Andreaus, U. (1996), "Failure criteria for masonry panels under in-plane loading", *J. Struct. Eng. - ASCE*, **122**(1), 37-46.
- ANSYS (Version 10), Online help and reference manual of ANSYS.
- Bakhteri, J., Makhtar, A.M. and Sambasivam, S. (2004), "Finite element modelling of structural clay brick masonry subjected to axial compression", *J. Teknologi*, **41**(B), 57-68.
- Bruneau, M. (1994), "State-of-the-art report on seismic performance of unreinforced masonry buildings", *J. Struct. Eng. - ASCE*, **120**(1), 231-251.
- Gidigasu, M.D. (1974), "Degree of weathering in the identification of laterite materials for engineering purposes – a review", *Eng. Geol.*, **8**, 213-266.
- Gumaste, K.S., Rao, N.K.S., Reddy, V.B.V. and Jagadish, K.S. (2007), "Strength and elasticity of brick masonry prisms and wallettes under compression", *Mater. Struct.*, **40**, 241-253.
- IS 1893 (2002), *Indian standard criteria for earthquake resistant design of structures*, Bureau of Indian Standards, New Delhi, India.
- IS 3620-1979 (Reaffirmed 1998), *Indian standard specification for laterite stone block for masonry*, Bureau of Indian Standards, New Delhi, India.
- IS 4326-1993, *Earthquake resistant design and construction of buildings – code of practice*, 2<sup>nd</sup> revision, Bureau of Indian Standards, New Delhi, India.
- Jagadish, K.S., Raghunath, S. and Rao, N.K.S. (2003), "Behaviour of masonry structures during the Bhuj earthquake of January 2001", *Proc. Indian Acad. Sci. (Earth Planet. Sci.)*, **112**(3), 431-440.
- Jhung, M.J. (2009), "Seismic analysis of mechanical components by ANSYS", Korea Institute of Nuclear Safety, KINS/RR-685.
- Karantoni, F.V. and Fardis, M.N. (1992), "Computed versus observed seismic response and damage of masonry buildings", *J. Struct. Eng. - ASCE*, **118**(7), 1804-1821.
- Kasturba, A.K. (2005), "Characterisation and Study of Weathering Mechanisms of Malabar Laterite for Building Purposes", Unpublished Ph.D. thesis, Dept. of Civil Engineering, IIT, Madras, India.
- Raghunath, S., Rao, K.S.N. and Jagadish, K.S. (2000), "Studies on The Ductility of Brick Masonry Walls with Containment Reinforcement", *Proc. 6<sup>th</sup> Int. Seminar on Structural Masonry for Developing Countries*, Bangalore, India.
- Raghunath, S. (2003), "Static and dynamic behaviour of brick masonry with containment reinforcement", Unpublished PhD thesis, Department of Civil Engineering, Indian Institute of Science, India.
- Sahin, A. (2010), "An seismic – a simple assistant computer program for implementing earthquake analysis of structures with ANSYS and SAP2000", *The Nineth International Congress on Advances in Civil Engineering (ACE 2010)*, Trabzon, Turkey.
- Saikia, B., Vinod, K.S., Raghunath, S. and Jagadish, K.S. (2006), "Effect of reinforced concrete bands on dynamic behavior of masonry buildings", *Indian Concrete J.*, 9-16, October.
- Sutapa, Das (2008), "Decay diagnosis of goan laterite stone monuments, 11 DBMC", *11<sup>th</sup> International Conference on Durability of Building Materials and Components*, Istanbul, Turkey.
- Tavarez, F.A. (2001), "Simulation of behavior of composite grid reinforced concrete beams using explicit finite element methods", Master's Thesis, University of Wisconsin, Madison, Wisconsin.
- Thakkar, K.S. and Agarwal, P. (2000), "Seismic Evaluation of Earthquake Resistant and Retrofitting Measures of Stone Masonry Houses", *12WCEE 12<sup>th</sup> World Conference on Earthquake Engineering*, Auckland, 0110 New Zealand.
- Unnikrishnan, S., Narasimhan, M.C. and Venkataramana, K. (2011), "Studies on uniaxial compressive strength of laterite masonry prisms", *Int. J. Earth Sci. Eng.* **4**(2), 336-350.

Vyas, Ch.U.V. and Reddy, V.B.V. (2010), "Prediction of solid block masonry prism compressive strength using FE model", *Mater. Struct.*, **43**(5), 719-735.

SA